3D Characterisation of Short Fatigue Crack in Ti 6246

S. Birosca[1], F. A. Garcia-Pastor[1], M. Karadge[1], J.Y. Buffiere[2] and M. Preuss[1]

[1]School of Materials, The University of Manchester, Manchester, United Kingdom;
[2]GEMPPM, INSA Lyon, Villeurbanne Cede, France.

soran.birosca@manchester.ac.uk

In the present study, fatigue crack propagation was imaged non-destructively in 3 dimensions during in-situ fatigue loading of Ti-6246 using X-ray microtomography on beam-line ID19 at the European Synchrotron Radiation Facility (ESRF). Phase contrast enabled the visualization of the two-phase microstructure and in combination with absorption contrast the crack growth was recorded in-situ during fatigue test. In order to obtain the crystallographic orientation of individual grains along the crack path a 3D EBSD volume was recorded subsequently. By combining both techniques it was possible to relate the crystallographic orientation of grains to crack arrest and accelerated crack propagation. It is shown that the lamellar grain orientation and morphology have a great influence on the crack diversion and deviation. Moreover, crack resistance of the alloy is investigated by means of EBSD grain characterisation methodology, orientation and misorientation data evaluations.

Keywords: Titanium alloy, X-ray tomography, EBSD, fatigue, microstructure.

1. Introduction

Ti-6246 is a high strength solid solution α+β Ti alloy used at relatively elevated temperature applications [1, 2]. As in any other Ti alloys, a wide range of microstructures can be obtained through controlling the thermomechanical processing route. For applications where damage tolerance is required, producing a fully lamellar microstructure enhances the fracture toughness [3,4]. Processing the material above the β-transus can produce such microstructure. In addition, the cooling rates applied at the end of such a process play a defining role in terms of lamellae width, colony size and shape. It is believed that the most influential microstructural parameter on the mechanical properties of a fully lamellar microstructure is the α colony size, because it determines the effective slip length [4]. A high cooling rate will result in small colony size or eventually in a basket weave structure, which will increase the yield stress of the material [3,4,5].

In general, when Ti alloys are subjected to fatigue, the mechanical properties are strongly affected by the microstructure and also the crystallographic texture of the material. It has been widely reported that fatigue crack initiation and growth is strongly influenced by the microstructure, grain size, grain orientation, grain boundary geometry, second phase, precipitates and porosity [6]. Liu Bin *et al*., reported that a coarse and inhomogeneous microstructure possesses a weak fatigue resistance [7]. Other studies showed that the colony microstructure in α+β Ti alloys exhibits the slowest crack growth rate while the

fastest rates are found in a fine-grained equiaxed microstructure [8,9]. Many of these aspects are related to the crystallographic anisotropy of the hcp crystal structure of the α phase with slip in the <11-20> direction (<a> slip) being significantly easier than slip in the <11-23> direction (<c+a> slip) [4]. In the case of fatigue strength, experimental studies showed that a fully transformed (lamellar α) microstructure has poorer low cycle fatigue resistance than an α +β annealed microstructure, with the fatigue properties of a bi-modal microstructure (equiaxed α with transformed β) being superior to a purely equiaxed microstructure [3,4,5,10].

The observation of a crack by conventional techniques such as optical or scanning microscopy on a sample surface may be misleading particularly for short cracks as the microstructure has a significant affect on the crack shape. In addition, when studying long cracks, crack path discontinuities can make it very difficult to directly observe crack closure and its disappearance in some areas within the microstructure. While such concerns might not be of significant importance when only recording fatigue data, they become crucial when trying to understand the underlying micromechanics. Here, x-ray tomography is capable of providing bulk structural information in 3D. Furthermore, substantial improvements in synchrotron sources and detector technologies have enhanced the spatial resolution of x-ray microtomography. Thereafter, the development of phase contrast tomographic imaging has increased the capacity to image low contrast systems [11,12,13].

In the present study short crack propagation in Ti-6246 with a fully lamellar microstructure has been investigated by means of in-situ fatigue testing using x-ray microtomography combined with post-mortem 3D Electron Backscatter Diffraction (EBSD) characterisation. This allowed detailed monitoring of the crack path, crack diversion, branching and arrest and relate these observations to the 3D microstructure, particularly β grain boundaries. Additional EBSD mapping of slices from the studied volume provided the necessary crystallographic information of lamellae along the crack plane in order to relate local crack propagation to crystallographic orientation.

2. Experimental Procedures

The alloy used in this study was powder metallurgical processed Ti-6246 (Ti-6Al-2Sn-4Zr-6Mo), which was provided by Rolls-Royce plc in an as-hipped condition. The reason for using PM-Ti-6246 in this work was the small β grain size of less than 100 μm in the as received condition, which allowed controlling the crack growth in small samples necessary for the synchrotron x-ray microtomography experiment. Since the as received material had a very fine lamellar microstructure, the material was first heat-treated in argon atmosphere above the β-transus (T = 960°C) for two hours followed by water quenching and an hour anneal at 875°C followed by furnace cooling. The aim of this two-stage heat treatment was to generate a lamellar microstructure coarse enough to be revealed during the x-ray tomography experiment. The final microstructure has a β grain size in the range of 100 μm and the α lamellae are arranged in basketweave morphology. The average width of the α lamellae was estimated to be 3-5μm sufficient to be resolved with the given resolution during the synchrotron x-ray tomography experiment.

Specimens were machined by Electro Discharge Machining (EDM) for the in-situ fatigue loading experiment. In order to grow a crack in a defined position a triangular notch (2 μm width, 100 μm long and 20 μm deep) was milled on the surface of the gauge centre using a Focused Ion Beam (FIB).

The microtomography experiment was carried out on beam line ID19 at the European Synchrotron Radiation Facility (ESRF), Grenoble, France. The experimental set-up for such study is described in detail elsewhere [11,12]. The energy used during the experiment was 35 KeV, which allowed obtaining sufficient transmission in the given sample. The targeted spatial resolution was 0.7 μm with a 2048x2048 CCD-FReLoN (Charge Coupled Device – Fast Readout Low Noise) detector in order to analyze cross section with a maximum diagonal size of 1.4 mm and visualize the lamellar microstructure. The distance between the specimen and the detector was fixed at 200 mm to have sufficient phase contrast, which enables the visualization of the two-phase microstructure. Tomographic imaging was carried out by interrupting the fatigue test after a certain number of cycles and every tomographic scan comprised a set of 1500 radiographs, recorded over a 180° rotation along the vertical axis. It is important to note from a fatigue point of view that a scan took about 1 hour while the sample was kept loaded at the maximum stress level. Each tomographic set was later reconstructed to a 3D volume using a three-dimensional extension of the conventional two-dimensional filtered back projection algorithm. This reconstruction method is described in [13].

The mechanical tests were undertaken in-situ with a compact fatigue-testing machine set on the beam line rotating stage. An X-ray transparent PMMA cylinder was used to transmit the load between the lower mobile grip and the fixed upper grip. The fatigue test was a tension - compression experiment run with a frequency of 25 Hz, a maximum stress of 460 MPa (considering an uncracked cross section) and a stress ratio of R = 0.1. The propagation of the crack was checked by repeatedly cycling the samples 1000 times followed by taking a radiograph of the notched region. If a significant change of the crack was detected in the radiograph, a tomographic scan was recorded. The tomographic scans were recorded between 7,000 – 27,000 fatigue cycles. The fatigue test was stopped before specimen failure, in order to examine the specimen by means of EBSD. The radiographic projections were reconstructed using Fourier transformation algorithms resulting in a resolution or 'voxel' size of 1.4 μm in the reconstructed 3D data. The image quality of the tomogram was further improved by using MATLAB code developed by the ESRF to remove ring artifacts. The 3D data were visualized and analyzed using commercials image processing software ImageJ and Amira. By measuring the crack dimensions from the tomograms it was possible to record the c/a crack ratio throughout the experiment, which varied between 0.7 and 0.9. It was also possible to determine the stress intensity factor through the experiment, which was 5.33 MPa$\sqrt{m}$ after 7,000 cycles and 15.71 MPa$\sqrt{m}$ after 27,000 cycles with overall crack growth rate of 8.25×10^{-09} m/cycle.

Following the tomography data analysis areas of interest within the fatigued sample were indentified for further EBSD analysis. All EBSD scans were carried out using a Sirion Field Emission Gun Scanning Electron Microscopy (FEG-SEM). The operating voltage used was 20 kV to obtain optimum quality of diffraction patterns. Working distances

were varied from 10 to 15 mm. The microscope is fitted with an HKL-EBSD system and the obtained data were analyzed using the Channel 5 software packages. Prior to the first EBSD examination on the surface, colloidal silica polishing was carried out for a minimum of 30 minutes just prior to insertion of the sample into the microscope. Subsequent EBSD scans were preformed 10, 30, 100, 150 and 250μm below the sample surface by removing material (conventional grinding and polishing) along the ND direction (see Fig. 1). This quasi-3D construction of an EBSD map was necessary to identify the crystallographic information from individual lamellae, which could not be obtained by x-ray microtomography. Since the microstructure of the sample had already been recorded during the x-ray microtomography scans it was possible to accurately align the EBSD maps with the tomograms and study for instance the impact of the crystallographic orientation of individual lamellae on local crack propagation.

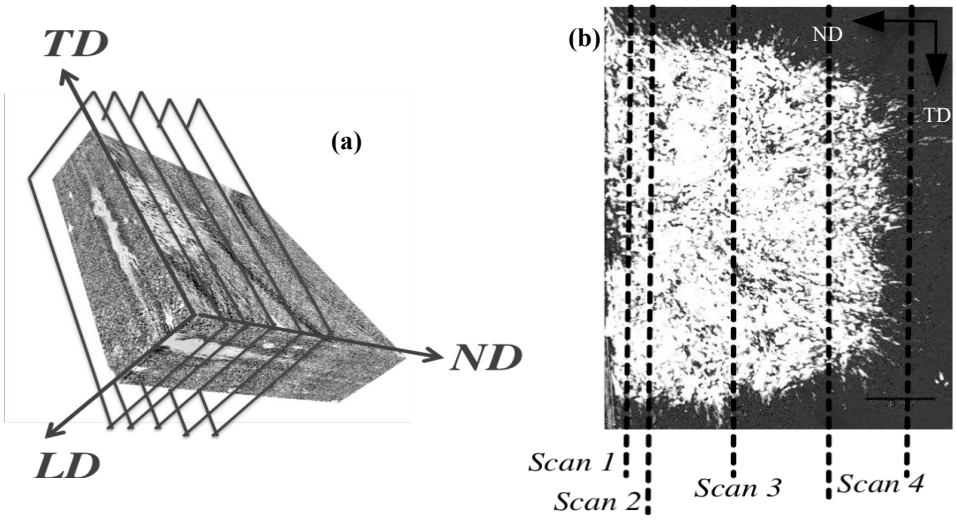

Fig. 1: The region of interests in the tomographic scans where the EBSD scans carried out on LD-TD surface along ND direction (a), the EBSD scan locations are shown on TD-ND surface (b).

3. Results and Discussions

Fig. 2a-c shows selected 2D slices of the three principles planes around the crack (looking down the crack growth direction, LD-TD-plane, Fig. 2a; crack from the side, ND-LD-plane, Fig. 2b; crack plane from the top, ND-TD-plane, Fig. 2c) taken from the tomogram after 27,000 cycles. Particularly from Fig. 2a and b it is possible to identify the prior β grain boundaries, which are now occupied by α grains. Fig. 2c shows a significant amount of artefacts near the crack tip, which is a result of the high level of phase contrast. The α lamellae microstructure is more difficult to identify and is only clearly revealed in some areas for a specific grey level and contrast settings. However, it was generally possible to study the interaction of crack tip line with the microstructure in 3D by changing the grey level for different positions.

In the case of metals with an hcp crystal structure, transgranular fracture will be greatly affected by the crystallographic orientation of grains with respect to the applied stress

axis due to the limited number of easy slip planes, whilst for intergranular failure the orientation of the boundary plane with respect to stress axis and the misorientation between the grains are critical [14]. Fig. 3 shows a SEM image (a) and a band contrast map (b) plotted from the EBSD scan recorded on the slice 10 μm below the original surface of the sample. The band contrast map is the best mode to visualise the crack in an EBSD map and at the same time visualise the morphology of the microstructure. Similar maps were plotted from all five EBSD scans recorded at different ND positions and they revealed that the majority of the crack propagation is of trans-lamellar nature with only few segments of the crack having grown parallel to the lamellar interface (referred to as inter-lamellar). This is in agreement with Huang *et al*., who found similar crack/morphology interaction in a fully lamellar microstructure [15].

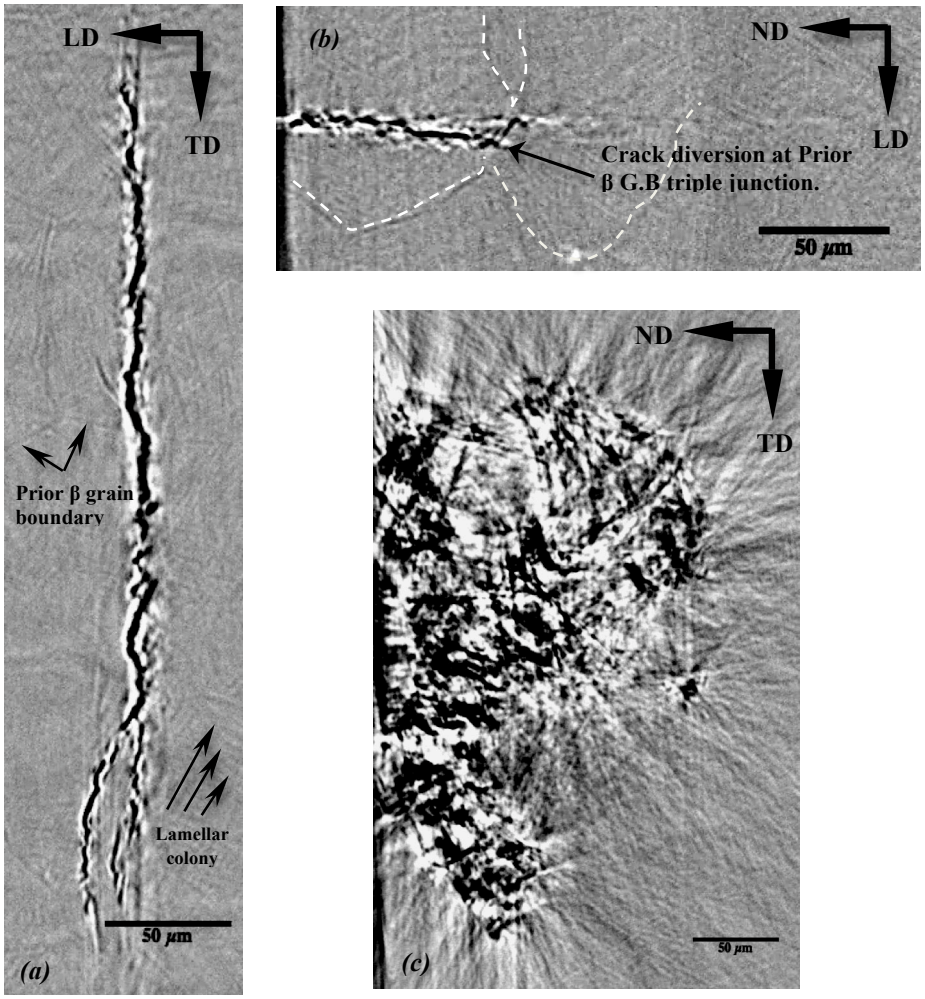

Fig. 2: X-ray tomography showing the crack shape after 27K fatigue cycles (LD: Loading axis Direction, TD: Transverse Direction and ND: Normal Direction).

Fig. 3a shows the effect of the lamellar grain boundary geometry on the crack path across the lamellar structure. As it can be seen from the same figure, in most cases the crack seems to cross the lamellar colonies at a 90° angle to the α/β interface. Therefore, even though macroscopically the crack appears to be a mode I crack as usually reported in the

literature [6,16,17], microscopically it seems to be a mode II crack interacting closely with the lamellar microstructure. Additionally, this observation was also confirmed by analysing the tomograms. Bache and Evans [18] also observed that the alpha colony morphology affects the crack growth direction. However, they did not find that the crack crosses favourably lamellae where the interface boundary is close to 90° as reported by Y.M. Hu *et al.* [6]. In terms of inter-lamellar crack growth, Kim and Laird [19] stated that cracking preferentially occurs if the trace of the lamellar boundary lies at an angle of 30-90° with respect of the loading direction. This orientation is assumed to provide a large driving force for the separation at the α/β lamellar interface within a colony. In contrast, Y.M. Hu *et al*. [6] argued that inter-lamellar cracking can occur at a random angle between the α/β boundary trace and the loading direction, even at an angle as small at 10°. Their findings suggest that apart from the applied stress, the internal stresses within individual colonies resulting from the crystallographic anisotropy and constraint during loading can play a significant effect on the inter-lamellar crack growth. For short crack propagation they agreed with Kim and Laid [19] that one of the favourable conditions for a short crack to propagate into the next grain/colony is that the microstructure allows the angle between the microcrack and the loading axis to be close to 90° [6]. Overall, there is uncertainty in correlating grain/lamellar boundary morphology and orientation to crack propagation although it seems to be clear that in two-phase titanium alloys the microstructure plays an important role in affecting the crack path. Consequently, it is important to identify the exact crystallographic orientation of the lamellae along the crack path and relate these to the loading direction. In addition, the crack growth might also be determined by grain boundary misorientation, which again requires detailed studies on the microstructural scale using EBSD as described in the following paragraphs.

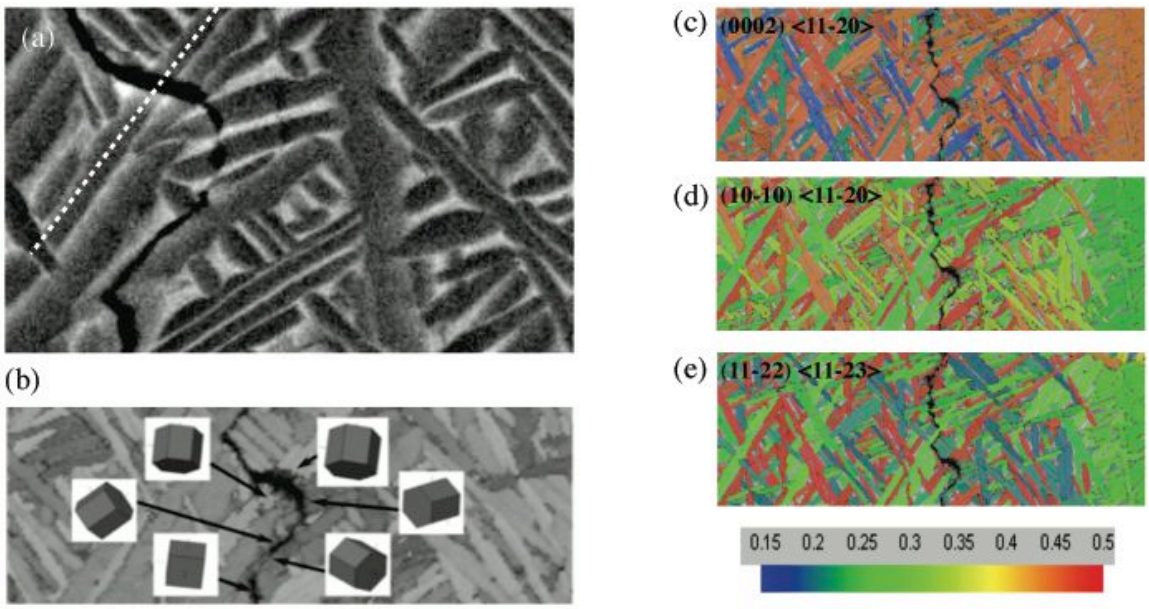

Fig. 3: (a) SEM image, (b) EBSD-derived band contrast map showing grain orientation effects on crack propagation direction (3D crystal viewer superimposed on the map), (c, d, e) EBSD-derived Schimd Factor maps for the same area in (a and b), the calculation carried out assuming the basal, prismatic and second-order pyramidal slip is activated as in c, d and e, respectively.

A small representative section from the map recorded at 10 μm below the original surface of the sample is shown in Fig. 3b. Along the crack path, schematic 3D hexagons have been added for some lamellae/colonies in order to better visualise the crystallographic orientation of these critical α grains. When closely inspecting Fig. 3b it can be seen that the crack has grown trans-lamellar in most cases and that the normal of the basal plane is close to a 90° angle to the crack. The effect of crystallographic orientation of the lamellar colonies on the crack propagation direction is evidence. As can be seen from the Fig. 3 (c, d and e), (see electronic version for colour images), the crack easily crossed the grain where favourably oriented for <a> basal slip. Whereas, the crack could not cross the grains where favourably oriented for prismatic slip, except in some cases. For instance, the lamellar grain indicated by a dashed line in Fig. 3a, where the crack has no other alternative route to cross. It is also clear that the crack has undulated (deviated) dramatically according to the lamellar orientation. As shown in the same figure, the crack could not cross most of the grains where favourably oriented for prismatic or pyramidal slips and it changed its direction to find an easier path where the basal slip is active. This explains the morphological feature of the crack in the SEM image in Fig. 3a, where the crack found to cross the lamellar colonies where their grain boundaries are close to 90° with the crack growth direction. Work by [10] has shown that when the c-axis of the hexagonal crystal is orientated perpendicular to the loading direction, greater plastic strain accumulation due to easy slip will lead to relaxation and therefore yield a better fatigue life than grains with the c-axis orientated along the loading direction. In the present study, statistical Schmid factor analysis of the EBSD maps showed that about 20% of the crack length showing trans-lamellar crack growth, had grains favourably orientated for prismatic slip while 80% were more likely to have undergone basal slip. From the current study, it seems to be clear that the crack requires a greater stress to propagate through a grain unfavourably oriented for <a> basal slip possibly leading to limited crack arrest when such a grain is encountered.

In addition, X-ray tomography data show that a more macroscopic type of crack diversion and bifurcation (Fig. 4) can be observed at locations of prior β grain boundary, see also Fig. 2 (a and b). Further analysis was needed and EBSD was employed to study this phenomenon in greater details. EBSD allows one to discriminate β (BCC) phase from α (HCP) phase if the regions of β phase are large enough to be detected by EBSD [20,21]. By recognising β phase in-between α lamellar colonies, the β grain orientation can be identified and represented in terms of an inverse pole figure, see Fig. 5a (IPF) map. The β grain shape can be detected from identifying the β grain boundary in a band contrast map. For better visualisation, the β grain boundary has been highlighted by thick black lines. Fig. 5a (Scan 2 in Fig. 1b) clearly shows that the crack diversion and bifurcation took place in the vicinity of prior β grain boundaries (see areas 1 and 2 in Fig. 5a). A more detailed visualisation of how the crack interacted with the prior β grain boundary was achieved by further polishing the sample along the ND direction (Fig. 1) until the crack bifurcation point was reached. Fig. 5b shows sections of 3 EBSD scans that were carried out until the crack bifurcation point was revealed. In Fig. 5b (I = scan 2 in Fig 1b), it can be seen that both branches of the crack are within one β grain. The steps of reaching the crack branching point are shown in (II = scan 3 in Fig. 1b) and (III = scan 4 in Fig. 1b). In (II), one branch shows clear discontinuities and has started to disappear,

which indicates that the point crack bifurcation is very close. It is clear form Fig. 5b (III), that the actual crack bifurcation has occurred at a prior β grain triple junction, where three or more β grains with different crystallographic orientation are meet. This was also observed from the tomography image in 3D (shown in the 2D LD-ND side surface image in Fig. 2b and Fig. 4b).

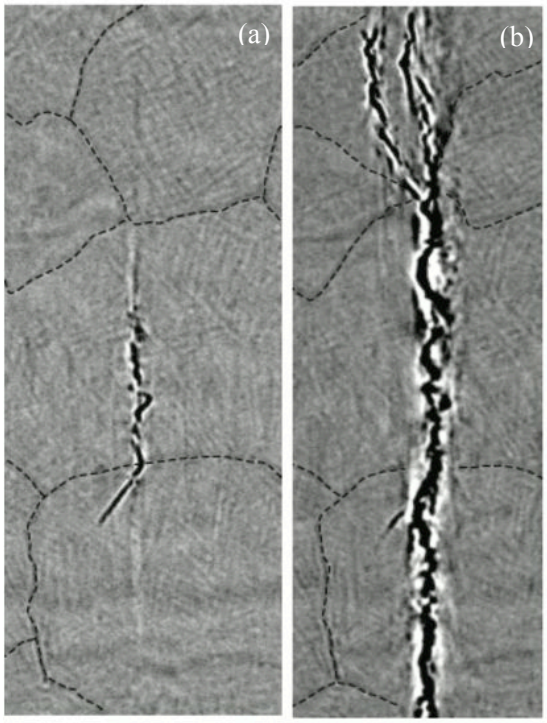

Fig 4: X-ray microtomography showing the crack diversion and bifurcation at β grain boundary and triple junction (a) at 7K and (b) at 27K.

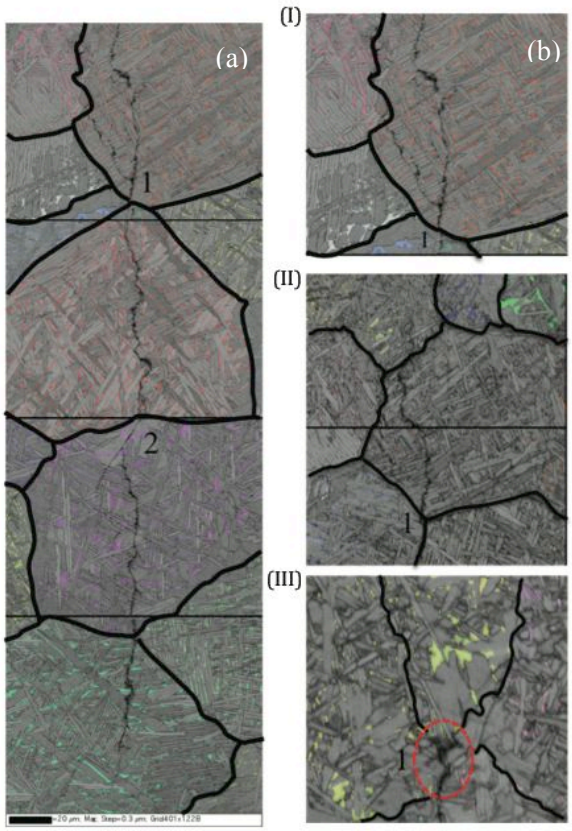

Fig 5: (a) EBSD- IPF map of the β phase with a superimposed Band Contrast map in order to visualise β grains and grain boundary α (Scan 2) (b) same type of map but I – III represent a 3D volume along the ND direction (I = scan 2, II = scan 3 and III – scan 4) visualizing the crack bifurcation at α triple junction.

In summary, the work has demonstrated that small crack undulation (deviation) can be related to lamellar (α colony) crystallographic orientation and morphology. This is in agreement with [22-25]. However, major crack diversion and bifurcation seems to be closely related to prior β grain boundary geometry, which might be somewhat surprising since grain boundary α is usually considered to be the weak part of a lamellar microstructure [26].

4. Conclusions

It has been shown in the present study for powder processed Ti-6Al-4V with a lamellar microstructure that crack propagation is largely affected by the crystallographic orientation of the α lamellae and the grain boundary β has the potential to divert and bifurcate the crack. The main findings of this work can be summarised as follows:

- Due to the phase contrast, synchrotron X-ray microtomography is capable of providing bulk microstructural information in 3D. It allows one to follow crack growth in 3D non-destructively and study the interaction of the crack with the microstructure.

- The prior β grain boundary interface seems to have the potential of diverting a crack and at prior β triple junctions to cause the crack to bifurcate.

- The fatigue crack path direction is greatly influenced by the α lamellar grain orientation and grain boundaries at a microscopic scale. In most cases the crack was found to cross the lamellar colonies where their grain boundaries were at a 90° angle with the crack growth direction.

- The crack was found to be diverted and possibly arrested when confronted by grains unfavourably oriented for basal <a> slip and favourably oriented for prismatic <a> and pyramidal <c+a> slip. This is not expected, as prismatic slip in the <a> direction should not be more difficult to activate than basal slip and <c+a> slip is known to have a substantially larger CRSS than <a> slip [4].

5. References

1. D. Bhattachayya, G.B. Viswanathan, R. Denkenberger, D. Furrer, H.L. Fraser. Acta Materialia (2003) 51:4679.
2. Jr M.J. Donachie. Titanium; A technical Guide, 2nd Edition, ASM International, The Materials Information Society, materials Park, Ohio, USA, (2000).
3. G. Lutjering., Materials Science and Engineering (1998) A243:32.
4. G. Lutjering, J.C. Williams. Titanium; Engineering Materials and Processes, 2nd Edition, Springer, Heidelberg, Germany (2007).
5. G. Schroeder, J. Albrecht, G. Luetjering. Materials Science and Engineering (2001) A319-321: 602.
6. Y.M. Hu, W. Floer, U. Krupp, H.J. Christ. Materials Science and Engineering (2000) A278:170.
7. L. Bin, L. Yong, H. Xiao-yu, T. Hui-ping, C. Li-Fang. Transactions of Nonferrous Metals Society of China (2008)18:227.
8. C. Sarrazin-Baudoux. International Journal of Fatigue (2005) 27:773.
9. C. Sarrazin, R. Chiron, S. Lesterlin, J. Petit. Fatigue & Fracture of Engineering Materials & Structure (1994) 17 (12):1383.
10. I. Bantounas, T.C. Lindley, D. Rugg, D. Dye. Acta Materialia (2007) 55:5655.

11. W. Ludwig, J.-Y. Buffière, S. Savelli, P. Cloetens. Acta Materialia (2003) 51 (3): 585.
12. M. Karadge, L. Babout, F. Garcia-Pastor, W. Ludwig, P.J. Withers, J.-Y Buffiere, M. Preuss. Conference Proceedings of Ti-2007, The Japan Institute of Metals, 239.
13. P. Cloetens, M. Pateyron-Salome, J.-Y Buffière, G. Peix, J. Baruchel, F. Peyrin, M. Schlenker. Journal of Applied Physics (1997) 81 (9):5878.
14. S.I. Wright, D.P. Field. Materials Science and Engineering (1998) A257:165.
15. Z.W. Huang, P. Bowen, P.A. Blenkinsop. Scripta Materialia (1998) 38 (7):1117.
16. K. Sadananda, A.K. Vasudevan. International Journal of Fatigue (2005) 27:1255.
17. F. Bridier, P. Villechaise, J. Mendez. Acta Materialia 2005;53:555.
18. M.R. Bache, W.J. Evans. Materials Science and Engineering (2001) A319-321:409.
19. W.H. Kim, C. Laird. Acta Materialia (1978) 26:777.
20. A.F. Gourgues. Materials Science and Technology (2002) 18:119.
21. S. Birosca, D. Dingley, R. L. Higginson. Journal of Microscopy (2004) 213 (3):135.
22. M Benedetti, V. Fontanari, G. Lutjering, J. Albrecht. Engineering Fracture Mechanics (2008) 75:169.
23. K.H. Khor, J.-Y Buffiere, W. Ludwig, I. Sinclair. Scripta Materialia (2006) 55:47.
24. M.R. Bache, W.J. Evans, B. Suddel, F.R.M. Herrouin. International Journal of Fatigue (2001) 23:S153.
25. M.R. Bache, W.J. Evans, V. Randle, R.J. Wilson. Materials Science and Engineering (1998) A257:139.
26. G. Lutjering, G. Source. Materials Science and Engineering A (2001) 319-321, 393.